Hydrology Research

British Hydrological Society

IWA PUBLISHING

Hydrology Research Vol 52 No 4, 944 doi: 10.2166/nh.2021.119

Regional water cycle response to land use/cover change for a typical agricultural area, North China Plain

Chang Li, Zhili Wang*, Yongjun Lu and Mingming Song

State Key Laboratory of Hydrology-Water Resources and Hydraulic Engineering, Nanjing Hydraulic Research Institute, Nanjing 210029, China
*Corresponding author. E-mail: zlwang@nhri.cn

ABSTRACT

Quantifying the influences of land use/cover (LULC) change on hydrological processes is important for rational utilization of water resources. The objective of this study was to evaluate the impacts of spatiotemporal LULC change on hydrological components in a typical agricultural area located in the North China Plain at both basin and sub-basin scales. LULC change was quantified, and the Soil and Water Assessment Tool was optimized using parameters associated with LULC conditions. We concluded that the urban and forest areas increased by 25.57 and 10.56%, with the cropland area decreased by 36.76%. About half of the surface runoff (SURQ) in the basin was generated from the urban area, with the SURQ increased significantly in the upstream and downstream of the basin where overlapped with urbanized areas. The proportions of evapotranspiration generated by cropland and forest areas increased slightly (0.89 and 0.55%, respectively), especially in sub-basins where the conversion of cropland to forest was obvious. Urban, forest, and cropland were the main types that generated water yield (WYLD). The proportion of WYLD generated on the urban area increased by 9.55% and decreased in other areas, which may be related to the combined effects of urbanization and forest reduction.

Key words: hydrological components, land use/cover change, scenario, SWAT

HIGHLIGHTS

- The SWAT model was used under different scenarios for a typical agricultural area, North China Plain.
- The influences of land use/cover change on key hydrological components were analyzed at both basin and sub-basin scales.
- Urbanization and reforestation will affect changes in hydrological components.

GRAPHICAL ABSTRACT

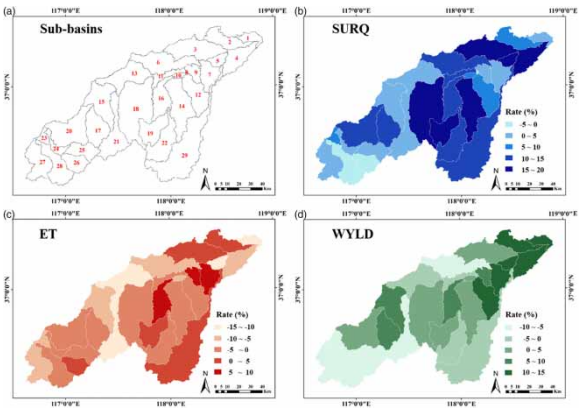

INTRODUCTION

Land use/cover (LULC) change is one of the most important drivers of ecohydrological changes (Blöschl *et al.* 2007; Li *et al.* 2009). Human economic activities represented by deforestation, reforestation, land reclamation, and urbanization alter land

cover status dramatically and affect the surface hydrological processes (Legesse *et al.* 2003; Mao & Cherkauer 2009; Wijesekara *et al.* 2012; Lejeune *et al.* 2014; Bai *et al.* 2018) and land–atmosphere interaction (Chu *et al.* 2010; Huang & Margulis 2010; Zhang *et al.* 2013). LULC change not only affects global environmental changes (Gedney *et al.* 2006; Bonan 2008), but also has a significant impact on the regional water cycle (Ruprecht & Stoneman 1993), and thus affect climate change indirectly (Zhang *et al.* 2013).

The natural circulation of water near the surface of the Earth includes several important parts: precipitation, evapotranspiration, infiltration, surface runoff (SURQ), and groundwater (Bari & Smettem 2004; Liu *et al.* 2008; Zucco *et al.* 2014; Chawla & Mujumdar 2015; Meng & Wang 2017). Human economic activities affect every part of the hydrological cycle by changing LULC patterns (Allen & Ingram 2002; Sandra & Sathian 2016). Thus, the effects of such developments on components of the hydrological cycle assume significant importance, especially for the rational utilization of water resources in agricultural areas.

Many studies have investigated the relationships between LULC patterns and hydrological processes (Wang *et al.* 2012; Liu *et al.* 2013; Zhang *et al.* 2013; Cheng *et al.* 2017). The results show that hydrological processes are affected not only by LULC types (Jian *et al.* 2015; Duan *et al.* 2016) but also by spatiotemporal heterogeneity (Chu *et al.* 2010; Liu *et al.* 2013). However, debate on the effects of LULC changes still exists due to the complex interaction between human activities and the hydrological cycle (Lørup *et al.* 1998; Alkama *et al.* 2013; Liu *et al.* 2016). In addition, many studies have estimated the hydrological response to LULC changes at the basin scale (Zhang *et al.* 2014, 2016a, 2016b; Cheng *et al.* 2017). Less attention has been paid to the spatiotemporal heterogeneity of the LULC change effects on hydrological components at the sub-basin scale.

Generally, there are two methodologies to assess the impact of LULC change on hydrology. One is based on paired catchment experiments. This approach is time-consuming and difficult to apply to large basins (Zuo *et al.* 2016). The other is constructing hydrological models to explore the response of the hydrological cycle to LULC changes under different scenarios (Bao *et al.* 2019). Brown *et al.* (2013) analyzed the impacts of vegetation changes on streamflow regimes based on this method and reported that impacts on low flows were greater than those on high and/or median flows. Many studies also focused on the effects of vegetation on hydrological components (Bosch & Hewlett 1982; Zhang *et al.* 2011). Among all the studies, the responses of different hydrological components to LULC changes and its spatiotemporal features have rarely been considered (Brown *et al.* 2005; Wang *et al.* 2012; Jian *et al.* 2015).

Hydrological modeling is a useful tool for evaluating the response of different hydrological components to LULC change (Yang *et al.* 2017; Lin *et al.* 2018; Zhi *et al.* 2018). The Soil and Water Assessment Tool (SWAT) model has been widely used for its ability to analyze the spatiotemporal heterogeneity of influence by considering topography, soil, land-use and other basin characteristics (Allen & Ingram 2002; Sandra & Sathian 2016; Meng *et al.* 2018). The accuracy of hydrological simulation will be greatly limited for basins lacking meteorological data. The China Meteorological Assimilation Driving Datasets (CMADS) (version 1.0) developed by the China Institute of Water Resources and Hydropower Research (IWHR) (Meng *et al.* 2018) can solve this problem with higher resolution and better accuracy. The datasets range from 2008 to 2016 and cover the entire East Asian region (Meng & Wang 2017). Some studies considered that CMADS + SWAT has better results for runoff simulation (Liu *et al.* 2018).

In this study, a novel framework was proposed to quantify the effects of LULC change on the hydrological components and analyze the spatiotemporal heterogeneity of the influences. First, the spatial and temporal differences in LULC change were analyzed in detail. Second, CMADS + SWAT was applied for hydrological simulation because the only three meteorological stations had a poor representation of the meteorological conditions in the study area. The SWAT model was calibrated and validated using parameters associated with different land cover maps. Third, different LULC scenarios were used to simulate the several phases of the hydrological cycle based on the SWAT model in the study area. The influences of LULC change on key components of the hydrological process were analyzed at both basin and sub-basin scales.

STUDY AREA AND DATA

Study areas

Xiaoqing River is one of the major rivers in the central area of Shandong Province, China. It originates from Jinan City and flows through Licheng, Zhangqiu, Zouping, Guangrao, Shouguang, and then into Laizhou Bay, Bohai Sea. The areas it flows through are all important agricultural areas in China. The Xiaoqing River Basin (XQB) has an area of 10,366 km^2 (116°30′–

118°45′E and 36°10′~37°30′N), with the elevation ranging from −12 m to 1,046 m (Figure 1). Flat topography characterizes most of the basin except for the southern mountains. The study region is dominated by the temperate monsoon climate, with an average annual temperature and average annual precipitation of 13.4 °C and 646.7 mm. About 50–70% of the annual precipitation is concentrated in June to September, and rainstorms generally occur in July and August. The total population in this region exceeds 27.4 million in 2017, with Jinan, the capital of Shandong Province, accounts for 34.10% of the total (Li *et al.* 2020). The main land-use types in this basin are forest (FRST), urban area (URBN), and cropland (AGRL), followed by water body (WATR), saline land (WETL), and barren land (BARR). Among them, the total area of forest, urban and cropland exceeds 85% (Li *et al.* 2020) of the total. The main soil types in the XQB are cinnamon soil and moist soil.

Data sources

The basic data used in this study are listed in Table 1 and described as follows:

1. The first version of the Advanced Spaceborne Thermal Emission and Reflection Radiometer (ASTER) Global Digital Elevation Model (GDEM) (grid cell: 10 m × 10 m) was used for sub-basin division, river system extraction, and slope reclassification.
2. Land-use data for 2010 and 2016 were interpreted from two cloud-free Landsat 8 OLI images with a resolution of 30 m and support vector machine algorithm. The LULC types include WETL, WATR, URBN, BARR, FRST, and AGRL (Figure 2).
3. The soil input data were obtained from the 1:1 million soil dataset created by the Cold and Arid Regions Sciences Data Center at Lanzhou. The spatial resolution of this soil database is 1 km × 1 km. The soil data were resampled before spatial analysis.
4. The meteorological data were taken from the CMADS version 1.0. This dataset include precipitation, temperature, relative humidity, solar radiation, wind speed, location, and the elevation of each site. Temperature, relative humidity, and wind speed were generated from 2,421 national automatic stations and 39,439 regional automatic stations. Precipitation data were generated from the integration of multiple satellite data and precipitation from ground automatic stations. The

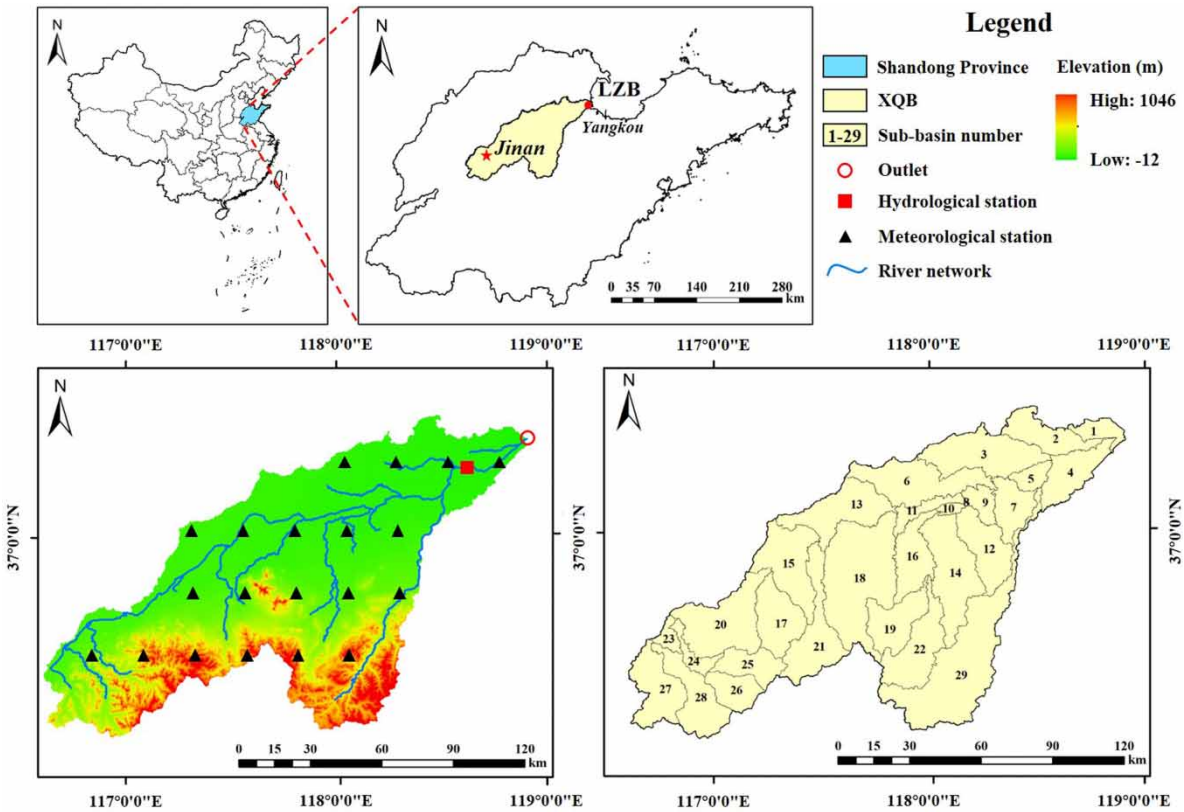

Figure 1 | River system, sub-basins distribution, and locations of meteorological and hydrological stations of the XQB.

Table 1 | Data description for the study area

Data type	Source	Spatial resolution
DEM	ASTER GDEM https://earthexplorer.usgs.gov/	10 m
Land use	Landsat-8 https://earthexplorer.usgs.gov/	30 m
Soil	HWSD http://westdc.westgis.ac.cn/data/	30 m
Weather	CMADS version 1.0 http://www.cmads.org/	28 km
Hydrological data	Nanjing Hydraulic Research Institute	–

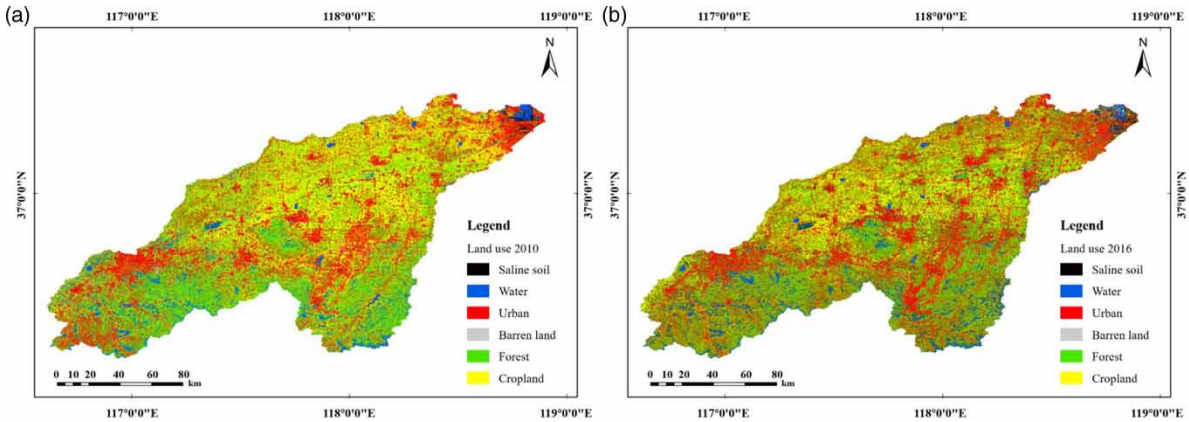

Figure 2 | LULC of the XQB in (a) 2010 and (b) 2016.

production of radiation data was based on the Discrete Ordinates Radiative Transfer (DISORT) radiative transfer model and the acquisition of products from the FY2E satellite primary product for inversion of solar shortwave radiation. Twenty CMADS meteorological stations were used in this study (Figure 1).

5. The hydrological data were provided by the Nanjing Hydraulic Research Institute and comprised measured monthly data from 2008 to 2016 at the Shicun Hydrological Station.

METHODS

LULC change detection

The transfer matrix reflects the conversion between land-use types in two periods quantitatively and directly by showing conversion source, destination, and quantity. The specific mathematical expression is shown as below:

$$S_{ij} = \begin{pmatrix} S_{11} & S_{21} & \cdots & S_{n1} \\ S_{12} & S_{22} & \cdots & S_{n2} \\ \cdots & \cdots & \cdots & \cdots \\ S_{1n} & S_{2n} & \cdots & S_{nn} \end{pmatrix}$$

where S_{ij} represents the area that was classified as land type i at the beginning of the study period (2010) and land type j at the end of the study period (2016). The sum of each column represents the percentage of land type i at the beginning of the study period converted into other land types at the end of the study. Row values represent all transfer types of land type j at the end of the study period.

Based on the land-use data generated from Landsat 8 OLI images, the LULC transfer matrix was calculated between 2010 and 2016. To analyze the spatial difference of LULC change, the conversions of land-use types were calculated at the sub-basin scale.

SWAT model setup, calibration, and validation

The SWAT model was developed by the U.S. Department of Agriculture (USDA) – Agricultural Research Services (ARS). It is a semi-distributed continuous hydrologic model (Arnold *et al.* 2012). The entire basin simulation domain is divided into sub-basins that are further subdivided into uniform hydrological response units (HRUs) with homogeneous soil, LULC, and slope characteristics. In this study, the XQB was divided into 29 sub-basins and 2,454 HRUs. The model parameters varies among different HRUs due to different land surface conditions. Theses parameters were determined through model calibration and validation. The simulation in this study was divided into three periods: warm-up period (2008–2009), calibration period (2010–2014), and validation period (2015–2016). Land-use data for 2010 were used for warm-up period and calibration period, while land-use data for 2016 were used for validation period.

Model calibration and parameter sensitivity analysis were conducted based on the SWAT Calibration and Uncertainty Program (SWAT-CUP). SWAT-CUP is a public domain program developed by Abbaspour (2007). The Sequential Uncertainty Fitting version 2 (SUFI-2) algorithm in SWAT-CUP was selected as the calibration algorithm due to the ideal performance in large basins (Rostamian *et al.* 2008). It provides a comprehensive optimization and uncertainty analysis through the global search method (Abbaspour 2014).

The SURQ was estimated by the modified Soil Conservation Service (SCS) Curve Number method (Neitsch *et al.* 2011). In this method, the amount of runoff was estimated based on local land-use types, soil types, and the antecedent soil moisture conditions. The Penman–Monteith method was used to estimate potential evapotranspiration effects. The physically meaningful absolute minimum and maximum ranges and fitted value for the key parameters involved in these methods were established (Table 2). Some studies focus on the analysis of parameter selection and sensitivity of the SWAT model (Cibin *et al.* 2010; Guse *et al.* 2013).

The coefficient of determination (R^2) and Nash–Sutcliffe Efficiency (NSE) were used to evaluate the performance of the SWAT model. The R^2 is squared Pearson correlation coefficient (R). NSE and R^2 are calculated as follows:

$$R^2 = \frac{\left[\sum_{i=1}^{n}(O_i - \overline{O})(P_i - \overline{P})\right]^2}{\sum_{i=1}^{n}(O_i - \overline{O})^2 \sum_{i=1}^{n}(P_i - \overline{P})^2}$$

$$\mathrm{NSE} = \frac{\sum_{i=1}^{n}(O_i - \overline{O})^2 \sum_{i=1}^{n}(P_i - \overline{P})^2}{\sum (O_i - \overline{O})^2}$$

Table 2 | Key SWAT model parameters and fitted values

Parameters	Variation	Min	Max	Fitted value	Rank
SOL_K	Relative	0	10	0.26	1
GW_REVAP	Replace	0.02	0.2	0.06	2
CN2	Relative	40	90	52.28	3
ESCO	Replace	0	1	0.53	4
ALPHA_BF	Replace	0	1	0.82	5
CH_K2	Replace	0	150	89.43	6
SOL_AWC	Relative	0	1	0.27	7
SURLAG	Replace	1	10	19.73	8
CH_N2	Replace	0.01	0.3	0.27	9
GWQMN	Replace	0	100	78.29	10
ALPHA_BNK	Replace	1	3	1.94	11
REVAPMN	Replace	0	50	38.67	12

Note: Relative means of an existing parameter value are simulated by the (1+ given value) and replace means the default parameter is replaced by the given value.

where $\overline{O}$ is the mean observed value, O_i is the ith observed value, P is the ith simulated value, $\overline{P}$ is the mean simulated values, and n is the total count of the sample pairs.

RESULTS AND DISCUSSION

LULC change

URBN, FRST, and AGRL were the primary land-use types in the XQB. The area of these three types accounted for 88 and 86% of the total area in 2010 and 2016, respectively (Table 3). The area of URBN and FRST showed upward trends totally. The area of URBN increased about 25.57% and its proportion of the total basin area has increased from 26% in 2010 to 32% in 2016. Similarly, the area of FRST increased about 10.56% and its proportion of the total basin area has increased from 30 to 34%. However, the area of AGRL decreased about 36.76% and its proportion of the total basin area has decreased significantly from 32 to 20%. The areas of WETL, WATR, and BARR remained relatively fixed in the study period.

To further analyze the change trajectory of main land-use types, the transfer matrices of URBN, FRST, and AGRL were calculated at the basin scale (Table 4). Overall, changes mainly occurred among these three types. About 23.57% of URBN converted to FRST and AGRL, and more than 19% of FRST converted to URBN and AGRL. Besides, nearly 50% of AGRL converted to URBN and FRST. These mainly be due to the relocation of towns in some southern mountainous areas and the implementation of 'Grain and Green' (Figure 2).

To identify the spatial and temporal differences of land-use change, the transferred matrix was also calculated at the sub-basin scale (Figure 3). The net conversion rate was calculated by the difference between conversion rates of two land-use types. The results showed that 6.78% of FRST and 10.27% of AGRL converted to URBN, respectively (Table 4). The sub-basins where AGRL/FRST converted to URBN were mainly distributed in the upper reaches (sub-basins 17, 20, 24, 27, and 28) and the lower reaches (sub-basins 1–5) of the whole basin. This is mainly due to the urbanization and population increase around Jinan City in the upper reaches and coastal areas recently (Li *et al.* 2020). In addition, 5.89% of AGRL converted to FRST in the XQB (Table 4). The conversion of AGRL to FRST occurred in most sub-basins (Figure 3). The results indicated that evident LULC changes may be due to the implementation of the 'Grain for Green' in the XQB.

Table 3 | LULC change in the XQB between 2010 and 2016

	Type											
	WETL		WATR		URBN		BARR		FRST		AGRL	
Year	Area	Pct.	Area	Pct.	Area	Pct.	Area	Pct.	Area	Pct.	Area	Pct.
2010	340.1	3	816.5	8	2,667.8	26	82.7	1	3,142.1	30	3,286.8	32
2016	672.8	7	662.5	6	3,349.9	32	98.2	1	3,473.9	34	2,078.5	20

Notes: The unit of area is km^2, Pct. is the abbreviation of percentage and its unit is %.

Table 4 | Primary patterns of LULC change in the XQB between 2010 and 2016

Conversion	Pct. (%)	Conversion	Pct. (%)
URBN to WETL	2.98	FRST to BARR	0.39
URBN to WATR	0.73	FRST to AGRL	18.82
URBN to BARR	2.17	AGRL to WETL	4.43
URBN to FRST	10.73	AGRL to URBN	23.11
URBN to AGRL	12.84	AGRL to WATR	1.31
FRST to WETL	2.87	AGRL to BARR	1.07
FRST to URBN	17.51	AGRL to FRST	24.71
FRST to WATR	4.89		

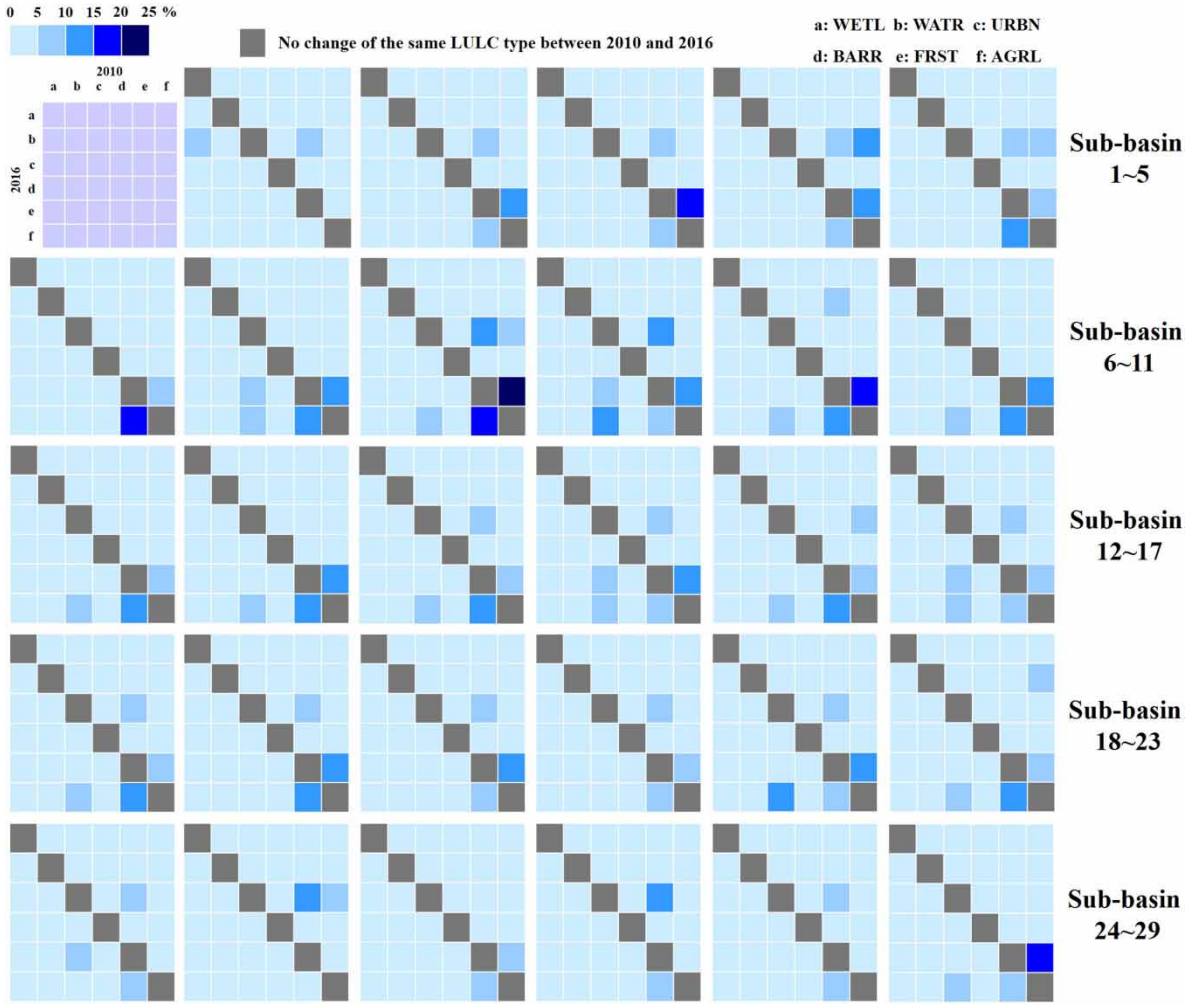

Figure 3 | LULC transfer matrices between 2010 and 2016 at the sub-basin scale.

Model performance analysis

The simulation result of monthly runoff from 2010 to 2016 in the XQB is shown in Figure 4. The R^2 and NSE for the calibration and validation periods were 0.81, 0.77 and 0.69, 0.60, respectively. Although the simulated result slightly underestimated streamflow in the dry period, the two statistical indexes (R^2 and NSE) indicated that the modeling accuracy was acceptable (Table 5).

Potential reasons for the underestimation can be categorized as measurement quality and model behavior. Measurement quality refers to missing precipitation data or streamflow measuring error. The study area is distributed in an agricultural plain region. Smaller slopes and larger amounts of river networks result in highly variable precipitation and difficulties in spatially estimating the precipitation (Jaepil *et al.* 2013). Additionally, considering the reduced accuracy caused by fewer meteorological stations in the XQB, the CMADS meteorological data were used for simulation (Figure 1). It has been reported that the accuracy of streamflow prediction mainly depends on the precipitation gage numbers and corresponding locations (Cao *et al.* 2006; Mul *et al.* 2009). Thus, the insufficient meteorological records and the distances among the meteorological stations result in limited simulation accuracy.

Model behavior refers to model limitations such as the inadequate representation of the physical mechanism of hydrological processes. For example, the SWAT uses total daily precipitation without considering rainfall intensity. Thus, runoff for some precipitation events (Qiu *et al.* 2012) can be estimated. Another example is the use of runoff curve

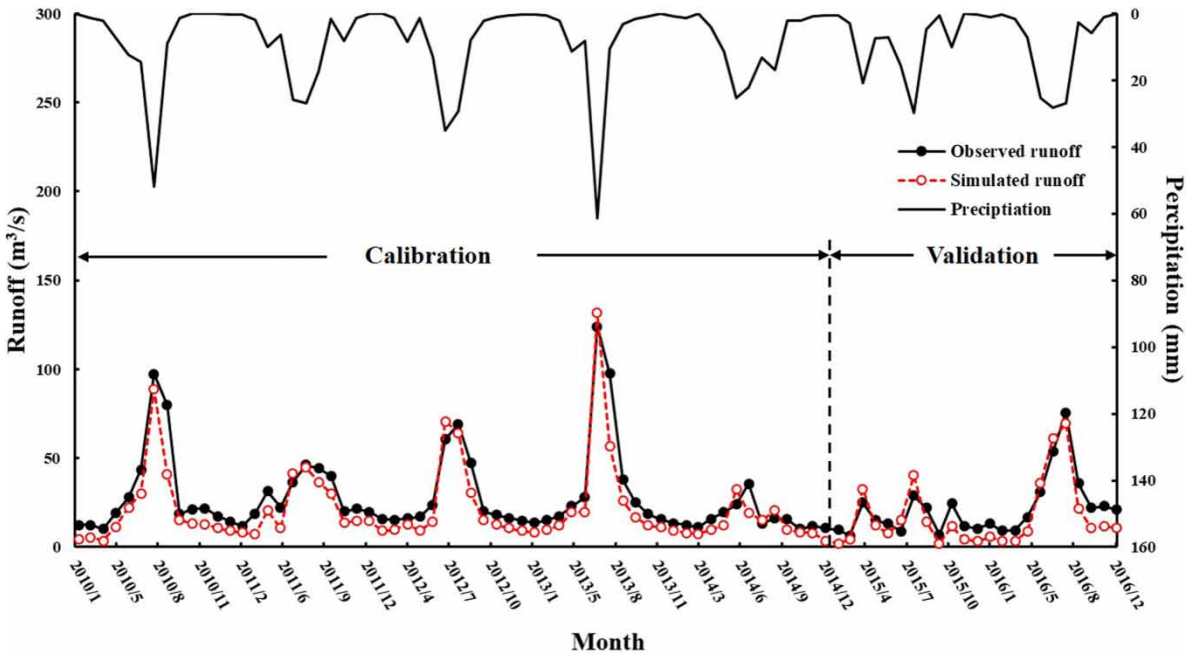

Figure 4 | Monthly precipitation and the simulated monthly runoff at the Shicun Station over the calibration (2010–2014) and validation (2015–2016) periods.

Table 5 | The performance of the SWAT model during the calibration and validation periods

Objects	Calibration (2009–2014)	Validation (2015–2016)
R^2	0.81	0.77
NSE	0.69	0.60

numbers to simulate the SURQ behavior. This approach does not account for saturation excess runoff or contributions from variable source areas (Garen & Moore 2005; Easton *et al.* 2008).

Temporal effects of LULC changes on hydrological components

Monthly runoff from 2010 to 2016 was simulated based on two LULC scenarios (2010LULC and 2016LULC) using the adjusted model. Three hydrological component indicators were analyzed: SURQ, ET, and WYLD. The total average values of these hydrological components were calculated (Figure 5(a)). SURQ increased by 49% and WYLD decreased by 47%, while ET remained relatively stable. The multi-year monthly average values of the hydrological components were also calculated (Figure 5(b)–5(d)). The hydrological components showed obvious seasonal variations, with high change values during July and August. SURQ increased 2.47–2.72 $\times 10^4$ mm in these two months under two LULC scenarios (Figure 5(b)) and WYLD increased 1.61–2.03 $\times 10^4$ mm (Figure 5(d)). The multi-year monthly average values of SURQ and WYLD under 2016LULC were 1.0–1.6 and 0.9–2.0 times of that under 2010LULC, respectively. However, there was little difference between the results of simulated ET under two scenarios (Figure 5(c)).

To further analyze the influences of different land-use types on the hydrological components, the proportions of hydrological components produced by different land-use types to the total amount of hydrological components were calculated (Table 6). URBN was the main type that generated SURQ under two scenarios. About half of the SURQ in the basin was generated from URBN. The expansion of the impervious surfaces caused by urbanization prevents water infiltration and brings more SURQ. From 2010 to 2016, the area of FRST increased from 3,142 to 3,473 km^2 (Table 3). The proportion of SURQ generated from FRST in the total amount of SURQ generated by all land-use types under two scenarios had decreased by 2.91%. The expansion of forest area has improved the capacity to conserve water in the study area.

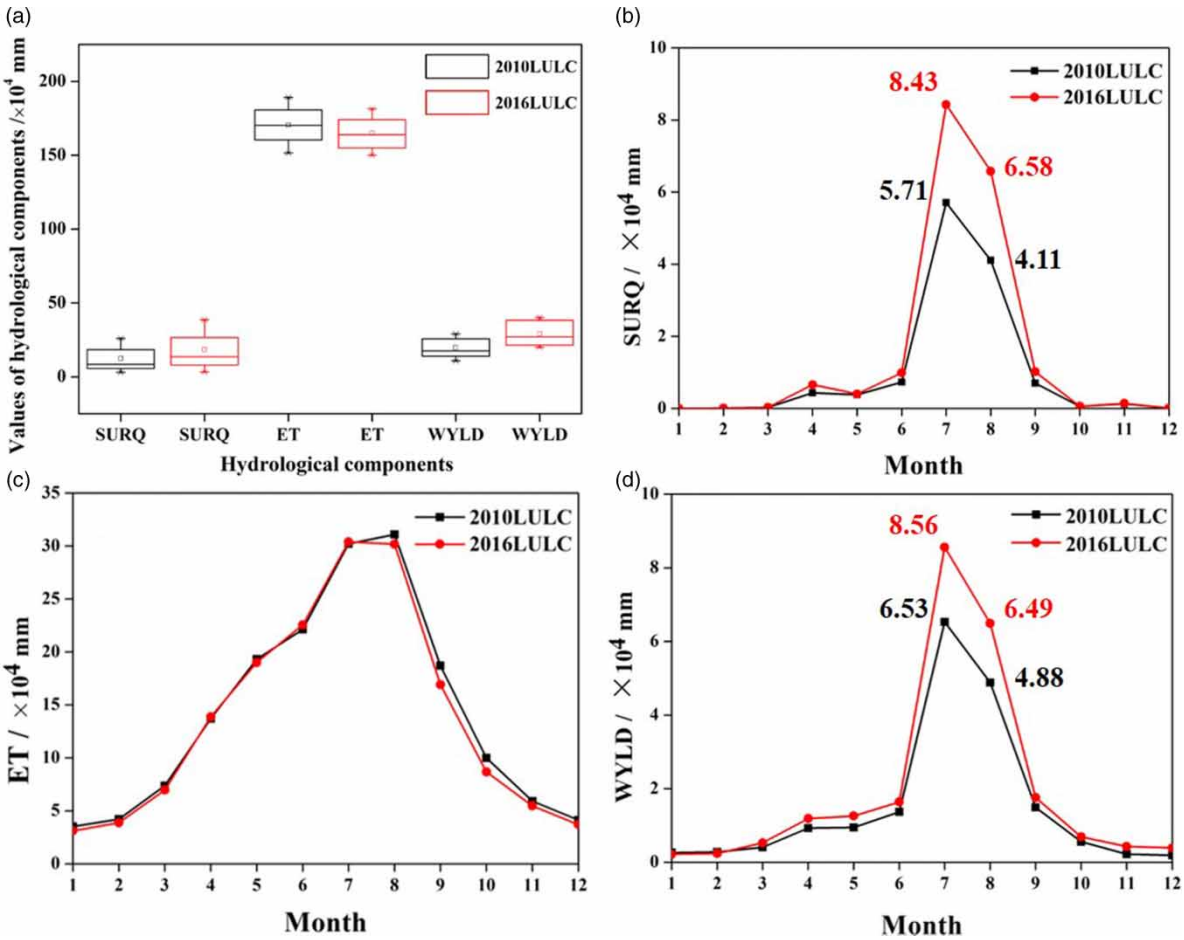

Figure 5 | The changes of hydrological components in the XQB under 2010LULC and 2016LULC. (a) Total average of SURQ/ET/WYLD. Multi-year monthly average values of (b) SURQ, (c) ET, and (d) WYLD.

Table 6 | proportions of SURQ/ET/WYLD on different LULC types under 2010LULC and 2016LULC

Components	Scenarios	AGRL (%)	BARR (%)	URBN (%)	FRST (%)	WATR (%)	WETL (%)
SURQ	2010LULC	14.70	11.18	44.62	15.14	0	14.36
	2016LULC	12.02	8.95	56.23	12.23	0	10.59
	Change	−2.68	−2.23	11.61	−2.91	0	−3.77
ET	2010LULC	12.41	9.45	11.07	12.89	42.03	12.16
	2016LULC	13.30	9.47	11.17	13.44	41.20	11.44
	Change	0.89	0.02	0.10	0.55	−0.84	−0.72
WYLD	2010LULC	15.30	11.57	42.29	15.79	0	15.04
	2016LULC	13.25	9.70	51.84	13.45	0	11.76
	Change	−2.05	−1.87	9.55	−2.34	0	−3.28

Moreover, WATR, AGRL, and FRST were the main land-use types that generate ET. From 2010 to 2016, the proportions of ET generated on AGRL and FRST in the total amount of ET generated by all land-use types had increased by 0.89 and 0.55%, respectively. Since the beginning of the 21st century, the policy of 'Grain for Green' has been gradually implemented, especially in Northern China (Schilling *et al.* 2018). Forests can store more water than cropland, and decrease streamflow and increase ET (Schilling *et al.* 2018) simultaneously. Meanwhile, about 5.89% of AGRL converted into FRST (Table 4). Therefore, under the same precipitation, more ET could be generated as the percentage of FRST increased from 2010 to 2016.

URBN, FRST, and AGRL were the main land-use types that generated WYLD. From 2010 to 2016, the WYLD generated on URBN in the total amount of WYLD generated by all land-use types had increased by 9.55%, with other land-use types showed decreasing trends. The influence mechanism of land-use on WYLD is complicated. In the SWAT model, WYLD is also related to SURQ, lateral flow, groundwater, and transmission losses in the shallow aquifer (Arnold *et al.* 1993). AGRL could hold the water in plants and soil. Meanwhile, crops need water to grow. FRST could transport water into the soil and produce lower WYLD (Im *et al.* 2003; Yang *et al.* 2013). In this study, the WYLD generated on FRST in the total amount of WYLD generated by all land-use types had decreased by 2.34% from 2010 to 2016, with the percentage of FRST area has risen by 4% (Table 3) in the same period. This was consistent with most previous studies (Bi *et al.* 2009), which suggested that forest may be an important factor for the WYLD.

Spatial effects of LULC changes on hydrological components

The spatial distribution of changes of ET, SURQ, and WYLD at the sub-basin scale is shown in Figure 6. SURQ increased more than 15% in some central and downstream parts of the whole basin, while minor increases occurred in some upstream sub-basins (e.g. sub-basins 17 and 20). ET increased obviously in the southern part and some upstream areas. The areas that were closed to the outlet also showed a 0.02–0.05% increase (e.g. sub-basins 2 and 3). As for WYLD, only some upstream parts (e.g. sub-basins 15 and 17) and the areas near the estuary (e.g. sub-basins 1 and 2) showed a significant increase, while other areas showed a downward trend, especially the southern parts of the whole basin.

Quantitative statistical analysis of the impacts of LULC changes on these hydrological components at the sub-basin scale is shown in Figure 7. The results indicated that the hydrological components varied among different LULC types in the whole basin.

URBN has the largest contribution rate to SURQ in the downstream part near the estuary and upstream part of the basin. Taking the sub-basin 20 close to Jinan City as an example, the SURQ generated on URBN has increased by more than 11%. A similar trend also occurred in sub-basin 4 (Figure 7). Numerous studies showed that urbanization alters a basin's response to

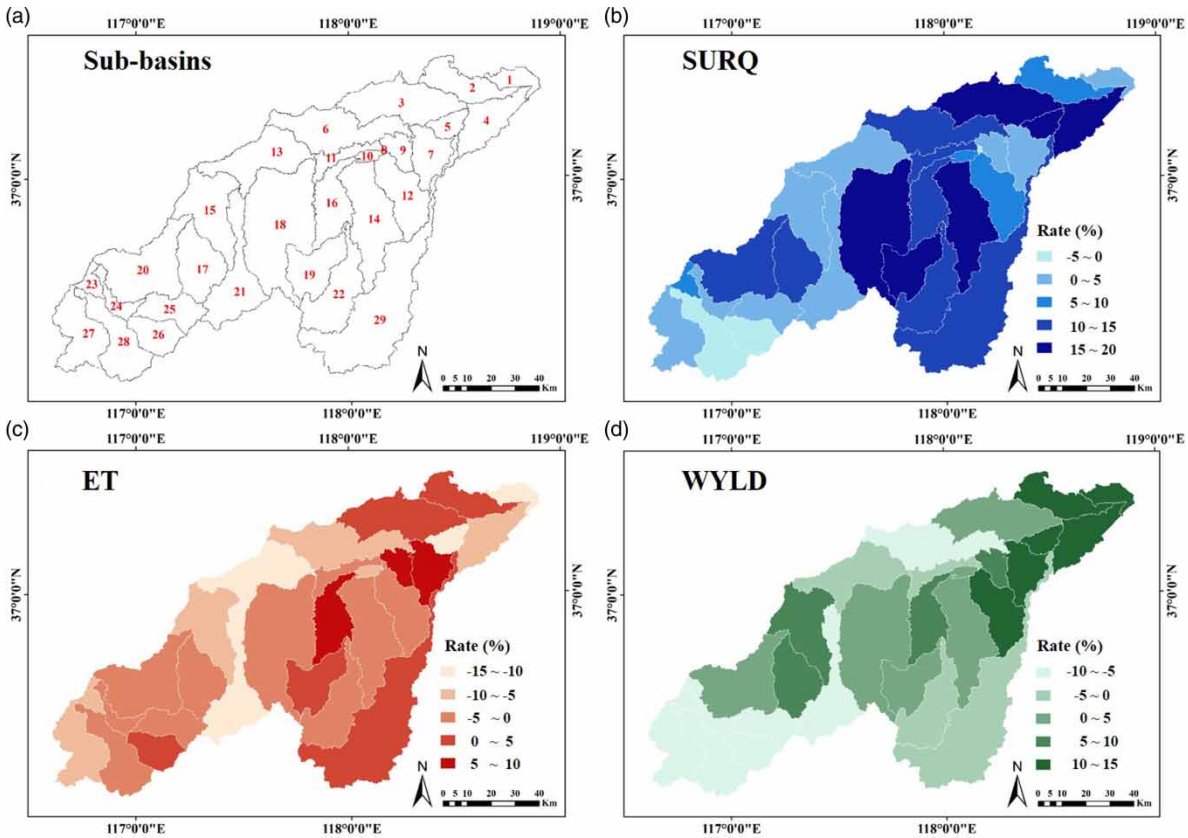

Figure 6 | Calculated hydrological component differences between 2010LULC and 2016LULC. (a) Sub-basin distribution, (b) SURQ, (c) ET and (d) WYLD.

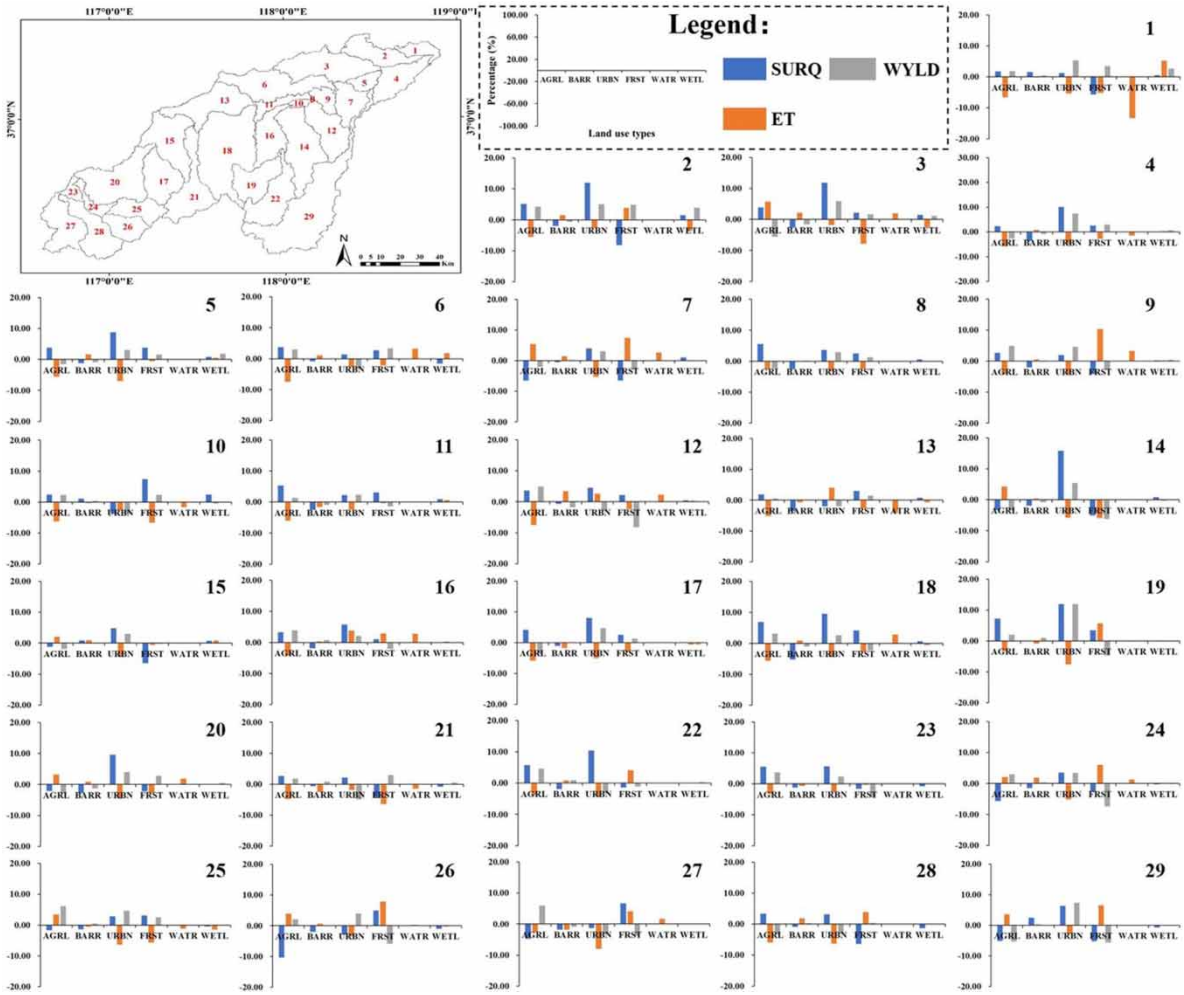

Figure 7 | The change of ET/SURQ/WYLD on different LULC types in each sub-basin.

precipitation events, leading to increased volumes of SURQ (McColl & Aggett 2007; Oudin *et al.* 2018; Li *et al.* 2020). In this study, the impervious areas expanded obviously due to the urbanization in the coastal areas and upstream areas. It leads to the weakening of the infiltration capacity of the ground and increasing the percentage of impervious surfaces (Cuo *et al.* 2008; Wang *et al.* 2012).

In contrast, ET showed a slightly decreasing trend in most areas of the XQB (Figure 6(c)). For example, ET generated on AGRL in sub-basin 18 decreased by 5.61% (Figure 7), where AGRL was the main land-use type. A similar trend also appeared in regions such as sub-basins 12 and 13. However, for FRST-dominated areas, the amount of ET increased as the area of FRST expanded. For example, the ET generated on FRST in sub-basin 29 increased by 6.53% and more than 15% of AGRL converted to FRST in the same sub-basin (Figure 3). Other studies reveal that ET rates from FRST are higher than other LULC types, generally due to their canopy interception and transpiration rates (Guse *et al.* 2013; Locatelli *et al.* 2017). In this study, the increasing trend of FRST in some sub-basins may be due to the implementation of the 'Grain for Green' policy that was mentioned above.

Numerous studies show that the combined effect of urbanization and forest reduction leads to an increase in WYLD, which may be due to an increase in direct runoff from impervious surfaces (Zhang *et al.* 2016a; Oudin *et al.* 2018). In the current study, the sum of WYLD generated on URBN and FRST increased about 10.43% in sub-basin 4, while that on AGRL decreased about 2.61% (Figure 7). From the perspective of the LULC transfer matrix (Figure 3), the combined increase of URBN and AGRL exceeded 20%, while the FRST decreased about 10% in the same region. Similar situations also can be seen in sub-basins 8 and 20 where urbanization and deforestation were obvious (Figure 3). These findings were consistent

with previous studies. Nevertheless, the process of WYLD was complicated, especially when other hydrological components changed, such as groundwater and lateral flow (Li *et al.* 2018). Previous studies showed that the change of WYLD is also related to such as climate change, regional differences, and soil conditions (Im *et al.* 2003; Li *et al.* 2018). Although the results of this study can reflect the general tendency of WYLD and reveal the relationship between WYLD and LULC to some degree, it is still necessary to further investigate in the future.

CONCLUSIONS

This study quantified the impacts of spatiotemporal LULC change on the water cycle at both basin and sub-basin scales in the XQB, a typical agricultural area located in the North China Plain. The SWAT model was used for monthly runoff simulation under two LULC scenarios. Both R^2 and NSE reached acceptable values in the calibration and validation periods. URBN, FRST, and AGRL were the dominant LULC types in the XQB. The land-use patterns changed significantly from 2010 to 2016. The urban and forest areas increased by 25.57 and 10.56%, with cropland area decreased by 36.76% from 2010 to 2016. From the perspective of net conversion rates, about 6.78% of FRST and 10.27% of AGRL converted to URBN, respectively. Besides, about 5.89% of AGRL converted to FRST in the XQB. These trends were closely associated with the development of urbanization and the implementation of the 'Grain for Green'.

The impacts of LULC change on hydrological components were also assessed quantitatively. Our analysis showed that SURQ has increased by 49% due to the expanded impervious surface area (25.57%) caused by the development of urbanization, especially in some upper and lower sub-basins. In other words, runoff increases as permanent imperviousness increases. There was little change of ET (−0.03%) under two LULC scenarios at the basin scale. However, ET increased in some sub-basins where the conversion of AGRL to FRST was obvious, which was the result of the implementation of 'Grain for Green'. For instance, ET increased by 6.53% in sub-basin 29, with 15% of the cropland area converted into forest. WYLD has increased by 47% from 2010 to 2016 at the basin scale generally. We roughly revealed that the increase of WYLD in some sub-basins was related to urbanization and forest reduction. These differences can explain the relationships between hydrological characteristics and LULC change at both basin and sub-basin scales to some extent.

In this study, the impacts of LULC change on the model performances were analyzed based on the calibrated results and uncertainty analysis of the model outputs. The significance of using dynamic land-use input instead of static land-use input when simulating hydrological components in a basin was revealed. This study can provide useful information for LULC planning and soil–water conservation in the agricultural area, North China Plain.

ACKNOWLEDGEMENTS

This study is funded by the National Key Research and Development Program of China (2018YFC1407601) and appreciates valuable comments and suggestions from editors and anonymous reviewers.

DATA AVAILABILITY STATEMENT

All relevant data are included in the paper or its Supplementary Information.

REFERENCES

Abbaspour, K. C. 2007 *User Manual for SWAT-CUP, SWAT Calibration and Uncertainty Analysis Programs*. Swiss Federal Institute of Aquatic Science and Technology, Dubendorf, Switzerland.

Abbaspour, K. 2014 *SWAT-CUP 2012: SWAT Calibration and Uncertainty Programs – A User Manual*. Swiss Federal Institute of Aquatic Science and Technology, Switzerland.

Alkama, R., Marchand, L., Ribes, A. & Decharme, B. 2013 Detection of global runoff changes: results from observations and CMIP5 experiments. *Hydrol. Earth Syst. Sci.* **17**, 2967–2979.

Allen, M. R. & Ingram, W. J. 2002 Constraints on future changes in climate and the hydrologic cycle. *Nature* **419**, 224–232.

Arnold, J. G., Allen, P. M. & Bernhardt, G. 1993 A comprehensive surface-groundwater flow model. *J. Hydrol.* **42**, 47–69.

Arnold, J. G., Moriasi, D. N., Gassman, P. W., Abbaspour, K. C., White, M. J., Srinivasan, R., Santhi, C., Harmel, R. D., van Griensven, A., van Liew, M. W., Kannan, N. & Jha, M. K. 2012 SWAT: model use, calibration, and validation. *Trans. ASABE* **55**, 1491–1508.

Bai, P., Liu, X. M., Zhang, Y. Q. & Liu, C. M. 2018 Incorporating vegetation dynamics noticeably improved performance of hydrological model under vegetation greening. *Sci. Total. Environ.* **643**, 610–622.

Bao, Z. X., Zhang, J. Y., Wang, G. Q., Chen, Q. W., Guan, T. S., Yan, X. L., Liu, C. S., Liu, J. & Wang, J. 2019 The impact of climate variability and land use/cover change on the water balance in the Middle Yellow River Basin, China. *J. Hydrol.* **577**, 123–136.

Bari, M. & Smettem, K. R. J. 2004 Modelling monthly runoff generation processes following land use changes: groundwater–surface runoff interactions. *Hydrol. Earth Syst. Sci.* **8**, 903–922.

Bi, H., Liu, B., Wu, J., Yun, L., Chen, Z. & Cui, Z. 2009 Effects of precipitation and landuse on runoff during the past 50 years in a typical watershed in Loess Plateau, China. *Int. J. Sediment Res.* **24**, 352–364.

Blöschl, G., Ardoin-Bardin, S., Bonell, M., Dorninger, M., Goodrich, D., Matamoros, D., Merz, B., Shand, P. & Szolgay, J. 2007 At what scales do climate variability and land cover change impact on flooding and low flows? *Hydrol. Process.* **21**, 1241–1247.

Bonan, G. B. 2008 Forests and climate change: forcings, feedbacks, and the climate benefits of forests. *Science* **320** (5882), 1444–1449.

Bosch, J. M. & Hewlett, J. D. 1982 A review of catchment experiments to determine the effect of vegetation changes on water yield and evapotranspiration. *J. Hydrol.* **55** (1–4), 3–23.

Brown, A. E., Zhang, L., McMahon, T. A., Western, A. W. & Vertessy, R. A. 2005 A review of paired catchment studies for determining changes in water yield resulting from alterations in vegetation. *J. Hydrol.* **310** (1–4), 28–61.

Brown, A. E., Western, A. W., McMahon, T. A. & Zhang, L. 2013 Impact of forest cover changes on annual streamflow and flow duration curves. *J. Hydrol.* **483**, 39–50.

Cao, W. Z., Bowden, W. B., Davie, T. & Fenemor, A. 2006 Multivariable and multi-site calibration and validation of SWAT in a large mountainous catchment with high spatial variability. *Hydrol. Process.* **20**, 1057–1073.

Chawla, I. & Mujumdar, P. P. 2015 Isolating the impacts of land use and climate change on streamflow. *Hydrol. Earth Syst. Sci.* **19**, 3633–3651.

Cheng, L., Zhang, L., Chiew, F. H. S., Canadell, J. G., Zhao, F. F., Wang, Y. P., Hu, X. Q. & Lin, K. R. 2017 Quantifying the impacts of vegetation changes on catchment storage discharge dynamics using paired-catchment data. *Water Resour. Res.* **53** (7), 5963–5979.

Chu, H. J., Lin, Y. P., Huang, C. W., Hsu, C. Y. & Chen, H. Y. 2010 Modelling the hydrologic effects of dynamic land use change using a distributed hydrologic model and a spatial land use allocation model. *Hydrol. Process.* **24**, 2538–2554.

Cibin, R., Sudheer, K. P. & Chaubey, I. 2010 Sensitivity and identifiability of stream flow generation parameters of the SWAT model. *Hydrol. Process.* **24**, 1133–1148.

Cuo, L., Giambelluca, T. W., Ziegler, A. D. & Nullet, M. A. 2008 The roles of roads and agricultural land use in altering hydrological processes in Nam Mae Rim watershed, northern Thailand. *Hydrol. Process.* **22** (22), 4339–4354.

Duan, L. X., Huang, M. B. & Zhang, L. D. 2016 Differences in hydrological responses for different vegetation types on a steep slope on the Loess Plateau, China. *J. Hydrol.* **537**, 356–366.

Easton, Z. M., Fuka, D. R., Walter, M. T., Cowan, D. M., Schneiderman, E. M. & Steenhuis, T. S. 2008 Re-conceptualizing the soil and water assessment tool (SWAT) model to predict runoff from variable source areas. *J. Hydrol.* **348**, 279–291.

Garen, D. C. & Moore, D. S. 2005 Curve number hydrology in water quality modeling: uses, abuses, and future directions. *J. Am. Water Resour. Assoc.* **41**, 377–388.

Gedney, N., Cox, P. M., Betts, R. A., Boucher, O., Huntingford, C. & Stott, P. A. 2006 Detection of a direct carbon dioxide effect in continental river runoff records. *Nature* **439** (7078), 835–838.

Guse, B., Reusser, D. E. & Fohrer, N. 2013 How to improve the representation of hydrological processes in SWAT for a lowland catchment – temporal analysis of parameter sensitivity and model performance. *Hydrol. Process.* **28**, 2651–2670.

Huang, H. Y. & Margulis, S. A. 2010 Evaluation of a fully coupled large-eddy simulation land surface model and its diagnosis of land-atmosphere feedbacks. *Water Resour. Res.* **46** (6), 666–669.

Im, S., Brannan, K. M. & Mostaghimi, S. 2003 Simulating hydrologic and water quality impacts in an urbanizing watershed. *J. Am. Water Resour. Assoc.* **39**, 1465–1479.

Jaepil, C., David, B., George, V., Richard, L. & Timothy, S. 2013 Multi-site evaluation of hydrology component of SWAT in the coastal plain of southwest Georgia. *Hydrol. Process.* **27**, 1691–1700.

Jian, S. Q., Zhao, C. Y., Fang, S. M. & Yu, K. 2015 Effects of different vegetation restoration on soil water storage and water balance in the Chinese Loess Plateau. *Agric. Forest Meteorol.* **206**, 85–96.

Legesse, D., Vallet-Coulomb, C. & Gasse, F. 2003 Hydrological response of a catchment to climate and land use changes in Tropical Africa: case study south central Ethiopia. *J. Hydrol.* **275** (1–2), 67–85.

Lejeune, Q., Davin, E. L., Guillod, B. P. & Seneviratne, S. I. 2014 Influence of Amazonian deforestation on the future evolution of regional surface fluxes, circulation, surface temperature and precipitation. *Clim. Dynam.* **44** (9–10), 2769–2786.

Li, Z., Liu, W., Zhang, X. & Zheng, F. 2009 Impacts of land use change and climate variability on hydrology in an agricultural catchment on the Loess Plateau of China. *J. Hydrol.* **377**, 35–42.

Li, S., Yang, H., Lacayo, M., Liu, J. & Lei, G. 2018 Impacts of land-use and land-cover changes on water yield: a case study in Jing-Jin-Ji, China. *Sustainability* **10** (4), 960–976.

Li, S., Wang, H. Q., Wang, G. Q., Peng, Y. B. & Han, Z. L. 2020 Study on relationship between non-point source pollution and precipitation in Xiaoqing River Watershed. *Water Resour. Hydrol. Eng.* **51** (1), 147–158 (in Chinese).

Lin, C., Ma, R. & Xiong, J. 2018 Can the watershed non-point phosphorus pollution be interpreted by critical soil properties? A new insight of different soil P states. *Sci. Total Environ.* **628–629**, 870–881.

Liu, M., Tian, H., Chen, G., Ren, W., Zhang, C. & Liu, J. 2008 Effects of land use and land-cover change on evapotranspiration and water yield in China during 1900–2000. *J. Am. Water Resour. Assoc.* **44**, 1193–1207.

Liu, M., Tian, H., Yang, Q., Yang, J., Song, X., Lohrenz, S. E. & Cai, W. J. 2013 Long-term trends in evapotranspiration and runoff over the drainage basins of the Gulf of Mexico during 1901-2008. *Water Resour. Res.* **49** (4), 1988–2012.

Liu, Y., Xiao, J., Ju, W., Xu, K., Zhou, Y. & Zhao, Y. 2016 Recent trends in vegetation greenness in China significantly altered annual evapotranspiration and water yield. *Environ. Res. Lett.* **11**, 094010.

Liu, J., Shangguan, D., Liu, S. & Ding, Y. 2018 Evaluation and hydrological simulation of CMADS and CFSR reanalysis datasets in the Qinghai-Tibet Plateau. *Water* **10**, 513.

Locatelli, L., Mark, O., Mikkelsen, P. S., Arnbjerg-Nielsen, K., Deletic, A., Roldin, M. K. & Binning, P. J. 2017 Hydrologic impact of urbanization with extensive stormwater infiltration. *J. Hydrol.* **544**, 524–537.

Lørup, J. K., Refsgaard, J. C. & Mazvimavi, D. 1998 Assessing the effect of land use change on catchment runoff by combined use of statistical tests and hydrological modelling: case studies from Zimbabwe. *J. Hydrol.* **205**, 147–163.

Mao, D. & Cherkauer, K. A. 2009 Impacts of land-use change on hydrologic responses in the Great Lakes region. *J. Hydrol.* **374** (1–2), 71–82.

McColl, C. & Aggett, G. 2007 Land use forecasting and hydrologic model integration for improved land use decision support. *Environ. Manage.* **84**, 494–512.

Meng, X. & Wang, H. 2017 Significance of the China meteorological assimilation driving datasets for the SWAT model (CMADS) of East Asia. *Water* **9**, 765–769.

Meng, X., Sun, Z., Zhao, H., Ji, X., Wang, H., Xue, L., Wu, H. & Zhu, Y. 2018 Spring flood forecasting based on the WRF-TSRM mode. *Teh. Vjesn.* **25**, 141–151.

Mul, M. L., Savenije, H. H. G. & Uhlenbrook, S. 2009 Spatial rainfall variability and runoff response during an extreme event in a semiarid catchment in the South Pare Mountains, Tanzania. *Hydrol. Earth Syst. Sci.* **13**, 1659–1670.

Neitsch, S. L., Arnold, J. G., Kiniry, J. R. & Williams, J. R. 2011 *Soil and Water Assessment Tool: Theoretical Documentation Version 2009*. Texas A&M University System, Texas, USA.

Oudin, L., Salavati, B., Furusho-Percot, C., Ribstein, P. & Saadi, M. 2018 Hydrological impacts of urbanization at the catchment scale. *J. Hydrol.* **559**, 774–786.

Qiu, L. J., Zheng, F. L. & Yin, R. S. 2012 SWAT-based runoff and sediment simulation in a small watershed, the loessial hilly-gullied region of China: capabilities and challenges. *Int. J. Sediment Res.* **27**, 226–234.

Rostamian, R., Jaleh, A., Afyuni, M., Mousavi, S. F., Heidarpour, M., Jalalian, A. & Abbaspour, K. C. 2008 Application of a SWAT model for estimating runoff and sediment in two mountainous basins in central Iran. *Hydrol. Sci. J.* **53** (5), 977–988.

Ruprecht, J. K. & Stoneman, G. L. 1993 Water yield issues in the Jarrah forest of south-western Australia. *J. Hydrol.* **150** (2), 369–391.

Sandra, G. & Sathian, K. K. 2016 Assessment of water balance of a watershed using SWAT model for water resources management. *Int. J. Eng. Sci. Res. Technol.* **5**, 177–184.

Schilling, K. E., Jha, M. K., Zhang, Y. K., Gassman, P. W. & Wolter, C. F. 2018 Impact of land use and land cover change on the water balance of a large agriculture watershed: historical effects and future directions. *Water Resour. Res.* **44**, W00A09.

Wang, S., Fu, B. J., Gao, G. Y., Yao, X. L. & Zhou, J. 2012 Soil moisture and evapotranspiration of different land cover types in the Loess Plateau, China. *Hydrol. Earth Syst. Sci.* **16**, 2883–2892.

Wijesekara, G. N., Gupta, A., Valeo, C., Hasbani, J. G., Qiao, Y., Delaney, P. & Marceau, D. J. 2012 Assessing the impact of future land-use changes on hydrological processes in the Elbow River watershed in southern Alberta, Canada. *J. Hydrol.* **412**, 220–232.

Yang, C. G., Yu, Z. B., Hao, Z. C., Lin, Z. H. & Wang, H. M. 2013 Effects of vegetation cover on hydrological processes in a large region: Huaihe river basin, China. *J. Hydrol. Eng.* **18**, 1477–1483.

Yang, X., Tan, L., He, R., Fu, G., Ye, J., Liu, Q. & Wang, G. 2017 Stochastic sensitivity analysis of nitrogen pollution to climate change in a river basin with complex pollution sources. *Environ. Sci. Pollut. Res.* **24** (34), 26545–26561.

Zhang, L., Zhao, F., Chen, Y. & Dixon, R. N. M. 2011 Estimating effects of plantation expansion and climate variability on streamflow for catchments in Australia. *Water Resour. Res.* **47**, W12539.

Zhang, P., Liu, Y. H., Pan, Y. & Yu, Z. R. 2013 Land use pattern optimization based on CLUE-S and SWAT models for agricultural non-point source pollution control. *Math. Comput. Modell.* **58** (3–4), 588–595.

Zhang, Y. F., Guan, D. X., Jin, C. J., Wang, A. Z., Wu, J. B. & Yuan, F. H. 2014 Impacts of climate change and land use change on runoff of forest catchment in northeast China. *Hydrol. Process.* **28** (2), 186–196.

Zhang, S. L., Yang, D. W., Jayawardena, A. W., Xu, X. Y. & Yang, H. B. 2016a Hydrological change driven by human activities and climate variation and its spatial variability in Huaihe Basin, China. *Hydrol. Sci. J.* **61** (8), 1370–1382.

Zhang, S. L., Yang, D. W. & Jayawardena, A. W. 2016b Quantifying the effect of vegetation change on the regional water balance within the Budyko framework. *Geophys. Res. Lett.* **43** (3), 1140–1148.

Zhi, X., Chen, L. & Shen, Z. 2018 Impacts of urbanization on regional nonpoint source pollution: case study for Beijing, China. *Environ. Sci. Pollut. Res. Int.* **25** (10), 9849–9860.

Zucco, G., Brocca, L., Moramarco, T. & Morbidelli, R. 2014 Influence of land use on soil moisture spatial-temporal variability and monitoring. *J. Hydrol.* **516**, 193–199.

Zuo, D., Xu, Z., Yao, W., Jin, S., Xiao, P. & Ran, D. 2016 Assessing the effects of changes in land use and climate on runoff and sediment yields from a watershed in the Loess Plateau of China. *Sci. Total Environ.* **544**, 238–250.

First received 14 August 2020; accepted in revised form 17 May 2021. Available online 9 June 2021